ASTFE
American Society
of Thermal and Fluids Engineers

3rd Thermal and Fluids Engineering Conference (TFEC)
March 4–7, 2018
Fort Lauderdale, FL, USA

TFEC-2018-21681

ANALYSIS OF LIQUID-GAS TWO-PHASE FLOW PRESSURE DROP SIGNATURE IN MINICHANNELS

Mehdi Mortazavi[1,*] & Seyed A. Niknam[2]

[1]Multiscale Thermal Fluids Laboratory, Western New England University, Springfield, MA, 01119, USA

[2]Western New England University, Springfield, MA, 01119, USA

ABSTRACT

In this paper, the liquid-gas two-phase flow pressure drop signatures are analyzed for minichannels. The two-phase flow pressure drops are measured in a 2mm$\times$1mm flow channel supplied with air and liquid water. The ranges of air and water flow rates represent operating conditions of proton exchange membrane (PEM) fuel cells. As a PEM fuel cell operates, chemical energy is converted into electrical energy with water and heat as byproducts. The produced water can pass through the gas diffusion layer (GDL), a porous layer in PEM fuel cell, and emerges on its surface within the flow channel. This causes liquid-gas two-phase flow in flow channels. In this study, liquid-gas two-phase flow pressure drops are measured in an ex-situ PEM fuel cell test section. The experimentally measure pressure drops are compared with three models of two-phase flow pressure drop. Comparing 108 experimentally measured pressure drop data points with models proposed by Saisorn and Wongwises [29], English and Kandlikar [24], and Mishima and Hibiki [28] revealed that the latter showed the best prediction capability with a mean absolute percentage error as low as 10%. Moreover, in this study the distribution of pressure signatures are plotted and analyzed.

KEY WORDS: PEM fuel cell, liquid-gas two-phase flow, pressure drop, two-phase flow, minichannel

*Corresponding Mehdi Mortazavi: mehdi.mortazavi@wne.edu

1. INTRODUCTION

Proton exchange membrane (PEM) fuel cells are efficient and pollutant free type of energy systems. Through the electrochemical reactions in anode and cathode, they generate electricity with heat and water as the byproducts. The water produced during the operation of the PEM fuel cell can pass through the gas diffusion layer (GDL), the porous layer in PEM fuel cell, and enters into the flow channel [1]. The porous structure of the GDL has a significant impact on water transport from the catalyst layer, where the electrochemical reactions occur, to the flow channels [2–4]. The water removal from the flow channel can be based on different mechanisms, depending on the gas flow rate and water production rate [5]. When the water removal rate is less than the water production rate, a water lens may form within the gas channel. As this lens grows, it can clog the flow channel and cease the transport of the reactants to the catalyst layer. This is referred to as channel flooding and has been reported to lower the performance of the cell [6–8]. The emergence of liquid water in PEM fuel cell flow channel causes liquid-gas two-phase flow.

Liquid-gas two-phase flow in PEM fuel cell can be studied through direct and indirect methods. The direct methods include studying liquid-gas flow within the flow channel through transparent cell [5, 8–14], neutron imaging [15, 16], X-ray microtomography [17, 18], or gas chromatography [19, 20]. The indirect method of studying liquid-gas two-phase flow in PEM fuel cell includes measuring the properties that are immediate results of liquid-water accumulation within the flow channel. Liquid-gas two-phase flow pressure drop is an appropriate property that can reveal information about the accumulation of liquid water in flow channel [21]. This is because the accumulated water resists the gas flow and therefore results in an added pressure drop along the flow channel.

While the single-phase pressure drop in fluids is well understood and prediction can be done over a wide range of operating conditions, the liquid-gas two-phase flow pressure drop is not well identified for researchers. The physics behind liquid-gas two-phase flow is complicated to be modeled based on simplified mathematical equations.

The two-phase flow pressure drop is the sum of frictional, gravitational and accelerational pressure drop:

$$\Delta P_{\mathrm{TP}} = \Delta P_{\mathrm{TP,F}} + \Delta P_{\mathrm{TP,G}} + \Delta P_{\mathrm{TP,A}} \tag{1}$$

The acceleration pressure gradient is expressed as:

$$-\left(\frac{dP}{dz}\right)_{\mathrm{TP,A}} = G^2 \frac{d}{dz}\left[\frac{v_{\mathrm{g}} x^2}{\alpha} + \frac{v_{\mathrm{f}}(1-x)^2}{(1-\alpha)}\right] \tag{2}$$

where mass flow quality, x, is defined as:

$$x = \frac{G_g}{G_g + G_f} \tag{3}$$

α is the void fraction and represents the gas hold-up in the liquid stream. As the liquid and gas superficial velocities are low in PEM fuel cell flow channels, the acceleration pressure drop is a negligible term of the overall two-phase flow pressure drop. The superficial velocity of the fluid is defined as the bulk velocity of the fluid flowing within the channel cross sectional area.

For an inclined channel with the inclination angle of ϕ, the gravitational pressure gradient can be expressed as

$$-\left(\frac{dP}{dz}\right)_{\mathrm{TP,G}} = \left[\alpha \rho_{\mathrm{g}} + (1-\alpha)\rho_{\mathrm{f}}\right] g \sin\phi \tag{4}$$

For horizontal channels the inclination angle will be zero and therefore, the gravitational pressure gradient will be zero too. In macrochannels, the gravitational pressure gradient is a dominant term which needs to be considered in overall two-phase flow pressure drop but in mini/micro-channels, the dominant impact of surface tension diminishes the gravitational effects. Therefore it can be concluded that for PEM fuel cell application that includes minichannels, the only two-phase flow pressure drop term that remains in the right hand side of Eq. 1 is the frictional two-phase flow pressure drop.

There are two common approaches in predicting the two-phase flow frictional pressure drop; homogeneous equilibrium model and separated flow model. In homogeneous equilibrium model the two-phase mixture is treated as a pseudo single phase fluid with properties weighted to the quality. This model has been proven to result in accurate predictions at higher mass qualities [22–24]. Therefore, this model has less prediction capability for PEM fuel cell application. In separated flow model, the two-phase frictional pressure drop is calculated based on the single-phase frictional pressure drop by applying a two-phase flow frictional multiplier, ϕ_{f}^2. This method was originally introduced by Lockhart and Martinelli in 1949 [25].

Table 1 Values of Chisholm parameter [27]

Two-phase flow characteristics	Chisholm's parameter C
Laminar liquid-laminar gas	5
Turbulent liquid-laminar gas	10
Laminar liquid-turbulent gas	12
Turbulent liquid-turbulent gas	21

$$\left(\frac{dP}{dz}\right)_{\mathrm{TP}} = \phi_{\mathrm{f}}^2 \left(\frac{dP}{dz}\right)_{\mathrm{f}} \tag{5}$$

where ϕ_{f}^2 is the two-phase frictional multiplier based on liquid and has been reported to depend on the flow pattern [26]. The Martinelli parameter, X, is defined as:

$$X = \left[\left(\frac{dP}{dz}\right)_{\mathrm{f}} / \left(\frac{dP}{dz}\right)_{\mathrm{g}}\right]^{\frac{1}{2}} \tag{6}$$

Chisholm [27] introduced the Chisholm parameter, C. This parameter is used to define the frictional multiplier:

$$\phi_{\mathrm{f}}^2 = \frac{\left(\frac{dP}{dz}\right)_{\mathrm{TP}}}{\left(\frac{dP}{dz}\right)_{\mathrm{f}}} = 1 + \frac{C}{X} + \frac{1}{X^2} \tag{7}$$

The concept behind the Chisholm correlation (Eq. 7) is that the two-phase flow frictional pressure drop is equal to the sum of the pressure drop for each of the phases of liquid and gas and the interaction between these two phases:

$$\left(-\frac{dp}{dz}\right)_{\mathrm{TP}} = \left(-\frac{dp}{dz}\right)_{\mathrm{f}} + \left(-\frac{dp}{dz}\right)_{\mathrm{g}} + C\left[\left(-\frac{dp}{dz}\right)_{\mathrm{f}}\left(-\frac{dp}{dz}\right)_{\mathrm{g}}\right]^{\frac{1}{2}} \tag{8}$$

The Chisholm parameter, C, gives a quantitative value to the interaction between two phases which is a function of flow regime. These values are listed in Table 1.

Different C correlations are proposed by different research groups. In this paper, liquid-gas two-phase flow pressure drops are measured in an ex-situ PEM fuel cell experimental setup. The measured pressures are then compared with three different C correlations proposed for minichannels. The pressure drop signatures are also analyzed based on comparing the distributions of pressure signatures during a certain time period after

initiation of experiments.

The three two-phase flow pressure drop models that have been compared in this study are proposed by English and Kandlikar [24], Mishima and Hibiki [28], and Saisorn and Wongwises [29]. Mishima and Hibiki [28] measured two-phase flow pressure drop of air and deionized water in capillaries with internal diameter between 1mm and 4mm. They observed that the C parameter is a function of internal diameter of the capillary and proposed two sets of C correlation for circular and rectangular capillaries. For circular cross section, they proposed $C = 21[1 - \exp(-333D)]$ and for rectangular they suggested $C = 21[1 - \exp(-319D_{\mathrm{h}})]$.

Saisorn and Wongwises [29] measured the frictional pressure drop of air and water in capillaries with diameters between 0.15 mm and 0.53 mm. They proposed a C correlation based on dimensionless numbers:

$$\psi = \frac{\mu_{\mathrm{f}} j_{\mathrm{f}}}{\sigma}, \lambda = \frac{\mu_{\mathrm{f}}^2}{\rho_{\mathrm{f}} \sigma D_{\mathrm{h}}}$$

$$C = 7.599 \times 10^{-3} \lambda^{-0.631} \psi^{0.005} Re_{\mathrm{fo}}^{-0.008}$$

English and Kandlikar [24] measured liquid-gas two-phase flow pressure drop in an ex-situ PEM fuel cell test section with 1.01 mm hydraulic diameter of the flow channel. They used air and water as working fluids. They modified the model proposed by Mishima and Hibiki [28] and suggested a new C correlation for PEM fuel cell application. For circular flow channels in PEM fuel cell, they proposed $C = 5[1 - \exp(-333D)]$ and for rectangular flow channel they proposed $C = 5[1 - \exp(-319D_{\mathrm{h}})]$. Mortazavi and Tajiri [30] conducted a comprehensive review on two-phase flow pressure drop models for the application of PEM fuel cell.

In addition to model comparison, the normal distribution of pressure signals are also analyzed in this study. The probability density function (PDF) for the normal distribution is defined as

$$f(x|\mu, \sigma) = \frac{1}{\sqrt{2\pi}\sigma} e^{-\frac{1}{2}\left(\frac{x-\mu}{\sigma}\right)^2} \tag{9}$$

where μ is mean and σ^2 is the variance.

2. EXPERIMENTAL SETUP

Liquid-gas two-phase flow pressure drops were measured in an ex-situ experimental setup of PEM fuel cell. The test section included two parallel flow channels, each 2mm wide and 1mm deep. The flow channels were machined on a 0.5 inch thick polycarbonate plate and Toray carbon paper (TGP-060) was inserted between the two polycarbonate plates. The GDL sample was treated with Polytetrafluoroethylene (PTFE) based on the procedure explained in [31]. The flow channels were 24 cm long, and the pressure drop was measured over the 20 cm length of the channel through 0.396 mm diameter holes in a polycarbonate plate. Deionized water was injected through two 250 $\mu\mathrm{m}$ diameter stainless steel capillaries (Upchurch-U111) into the flow channels. Pressure drop was acquired at 50 Hz frequency with a high-precision pressure transducer 0-500 Pa (Omega, PX653-02D5V). The uncertainty associated with the pressure transducer was ± 0.25Pa. Table 2 lists the experimental conditions of this study. The Reynolds number in this table was calculated based on the superficial velocities of air or water. Figure 1 shows the schematic of experiments setup used in this study.

Table 2 Experiment conditions

Property	Air	Water	Mixture
Mass flux ($\mathrm{kg/m^2s}$)	1.36-5.44	0.04-0.45	1.56-5.78
Superficial velocity (m/s)	1.13-4.52	4.4×10^{-5}-4.53×10^{-4}	-
Reynolds number	96.0-385.3	0.063-0.654	-
Mass Flow Quality, x	-	-	0.869-0.986

3. RESULTS AND DISCUSSION

In this section experimentally measured two-phase flow pressure drops are first compared with three separated flow models that have been proposed for minichannels. The pressure drop signatures are also analyzed by

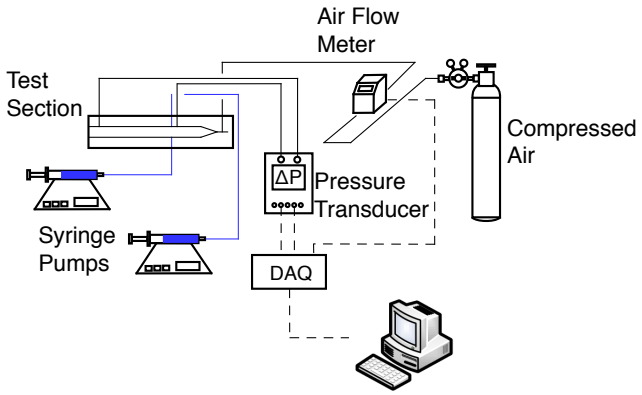

Fig. 1 Experimental setup

studying the normal distribution during the first and the third 100s, i.e. $0\text{s} < \text{time} < 100\text{s}$ and $200.02\text{s} < \text{time} < 300\text{s}$, respectively. Fig. 2 compares the experimentally measured two-phase flow pressure drops with the three models. In each graph, the horizontal axis represents the experimentally measured two-phase flow pressure drop and the vertical axis belongs to predicted two-phase flow pressure drop. A 30% margin for each model is also provided on each graph. It should be added that the two-phase flow pressure drops presented in Fig. 2 are the average values of pressure drop data after the pressure signatures passed the initial increasing trend, as discussed in Fig. 3.

In order to compare the accuracy of different models, four different parameters of λ, ω, θ, and ε were defined. The mean absolute percentage error (MAPE) is shown by λ which is determined according to

$$\text{MAE} = \frac{1}{\text{N}}\Sigma\frac{|\Delta P_{\text{F,pred}} - \Delta P_{\text{F,exp}}|}{\Delta P_{\text{F,exp}}} \times 100\% \tag{10}$$

Also, ω, θ, and ε are defined as the percentage of data points predicted within $\pm 10\%$, $\pm 30\%$, and $\pm 50\%$ of accuracy, respectively.

It can be observed from Fig. 2 that while the model proposed by Saisorn and Wongwises [29] generally over-predicts the pressure drop, the model proposed by English and Kandlikar [24] under-predicts the pressure drop. Fig. 2 also shows that the model proposed by Mishima and Hibiki [28] has the best prediction capability with the lowest MAPE, $\lambda = 10.0$. Another general observation from this figure suggests that the model proposed by Saisorn and Wongwises [29] has relatively better prediction capability at lower pressure drops while the model proposed by Mishima and Hibiki [28] has stronger prediction capability at higher pressure drops.

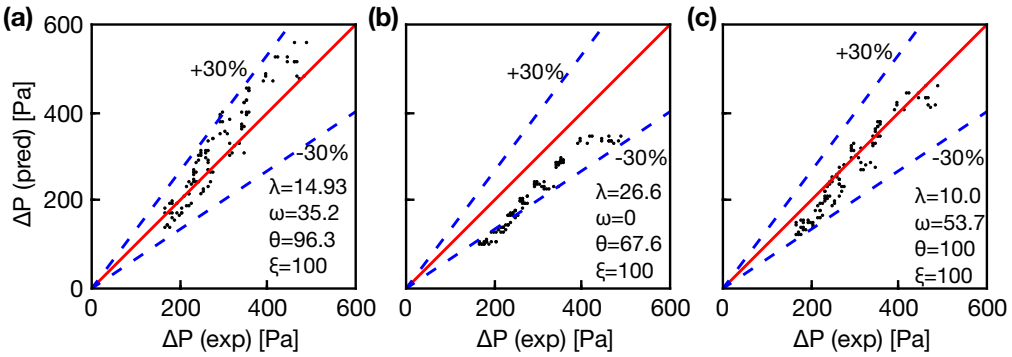

Fig. 2 Experimentally measured two-phase flow pressure drops compared with different models. (a) Saisorn and Wongwises [29], (b) English and Kandlikar [24], (c) Mishima and Hibiki [28]. 108 experimentally obtained data points are evaluated in this study.

In addition to lower MAPE calculated for Mishima and Hibiki's model [28], it can be observed from fig 2 that all data points are within 30% accuracy of this model. This percentage is 96.3% for the model proposed by Saisorn and Wongwises [29] and 67.6% for English and Kandlikar's model [24].

In addition to model comparison, the pressure drop signatures were analyzed by fitting to normal distribution at different time intervals. Fig. 3 shows the two-phase flow pressure drop signatures at five different water flow rates. For each water flow rate, experiment starts with dry channel and the pressure drop measured at time = 0s represents the single-phase air pressure drop along the flow channel. It can be observed in Fig. 3b that as the water flow rate increases, the pressure signature increases with a greater slope at the beginning of the experiment. This is due to a higher rate of water introduction into the flow channel that causes higher pressure drop at a shorter period of time. In addition, a closer look at three graphs in this figure shows that as the water flow rate increases, the changes in pressure signature between spikes and dips become faster.

Fig. 4 compares the PDFs for different water flow rates and during the first 100 s (Fig. 4a) and the third 100

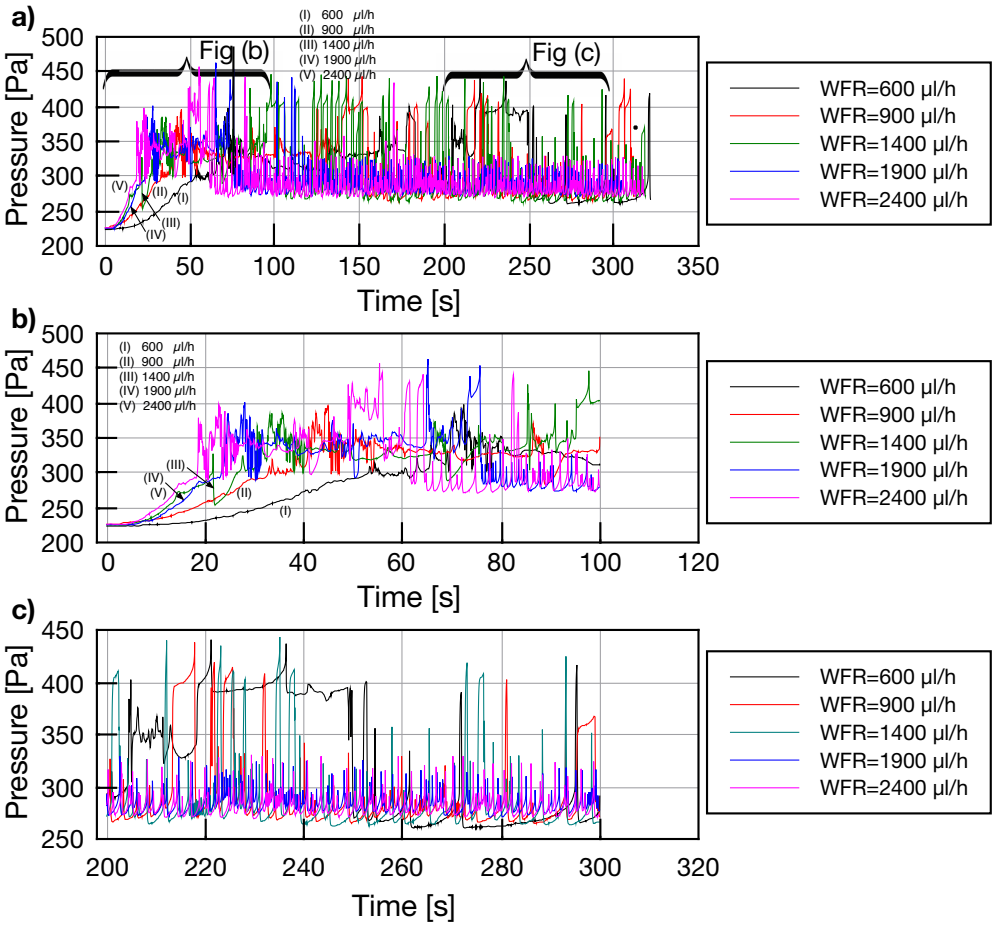

Fig. 3 Two-phase flow pressure drop signatures

s (Fig. 4b) of each experiment. While the PDF are relatively similar in shape in Fig. 4a, it can be observed that changing water flow rate changes the mean value of the pressure drop. In Fig. 4a, as the water flow rate increases the distributions shift to the right, suggesting an increase in the mean value of pressure drop at higher water flow rates.

Fig. 4b shows the PDFs of pressure signatures during the third 100 s of the experiments which is equivalent to time between 200.02 s and 300 s. A discernible trend can be observed in this figure that suggests as the water flow rate increases, the standard deviation of pressure signatures decreases. Based on test of hypothesis, the difference between two means of pressure drop for $600\mu\ell/h$ and $2400\mu\ell/h$ are statistically significant.

For the highest water flow rate, $2400\mu\mathrm{l/h}$, a jump in the PDF can be observed in Fig. 4b. This suggests a smaller standard deviation in pressure signature at this high water flow rate compared to lower water flow rates.

This study is a basic statistical analysis of pressure signatures and suggests that pressure signature can be further studied statistically. Further statistical analysis of pressure drop signals are required to learn more about the frictional pressure drop caused by the interaction between liquid and gas phase in PEM fuel cells.

4. CONCLUSION

In this study, liquid-gas two-phase flow pressure drop was measured in a minichannel. The measured two-phase flow pressure drops were compared with three models proposed for minichannels. The following conclusions can be drawn from this study:

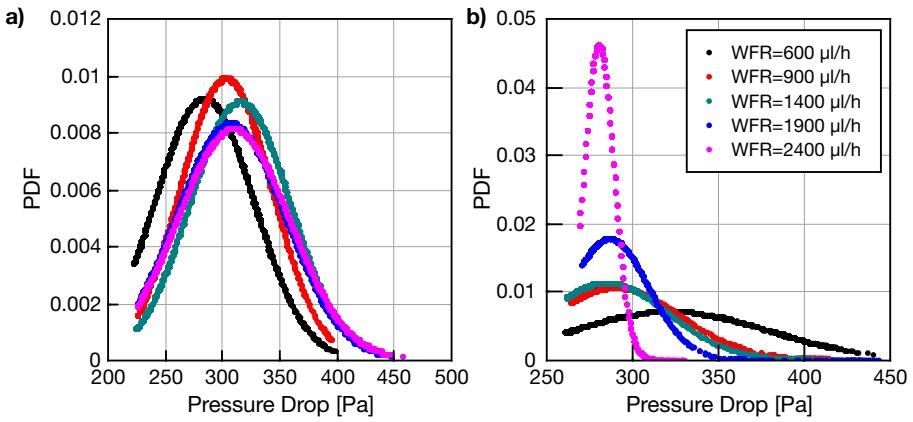

Fig. 4 Probability distributions drawn for (a) the first 100 s (b) the third 100 s of experiments. Legend applies to both figures.

1. Over the range of flow conditions tested in this study, it was observed that the model proposed by Mishima and Hibiki [28] has the strongest prediction capability compared to the two other models evaluated.

2. While the model proposed by Saisorn and Wongwises [29] generally over-predicts the value of pressure drop in the range of flow condition tested in this study, the model proposed by English and Kandlikar [24] was observed to under-predict values of pressure drop.

3. Comparing the model proposed by Saisorn and Wongwises [29] and the model proposed by Mishima and Hibiki [28], the former was observed to be more accurate at lower pressure drops (around 200 Pa) while the latter was observed to be more accurate at higher pressure drop (around 400 Pa).

4. The normal distributions of pressure signatures at different water flow rates showed that while the standard deviation was almost constant during the first 100 s of the experiments (Fig. 4a), the mean value of pressure drop increased with water flow rate. However, the standard deviation was observed to decrease during the third 100 s of experiments (Fig. 4b) as the water flow rate increased. In addition, increasing water flow rate was observed to decrease the mean value of pressure drop during the period of this plot. Further statistical analysis is required to learn more about the interaction of liquid and gas phase in the overall two-phase flow pressure drop equation.

ACKNOWLEDGMENTS

Western New England University is gratefully acknowledged for providing the startup fund for this research. The authors also would like to thank Peter Bennett for fabricating the test section used in this study.

NOMENCLATURE

C	Chisholm Parameter	(-)
D	Channel diameter	(m)
D_h	Channel hydraulic diameter	(m)
G	Mass flux	$(\frac{kg}{m^2 s})$
j_f	Superficial liquid velocity	(m/s)
j_g	Superficial gas velocity	(m/s)
N	Number of data points	(-)
N_{conf}	Confinement number	(-)
P	pressure	(Pa)
Re	Reynolds number	(-)
Re_f	Reynolds number based on superficial liquid velocity, $Re_f = G(1-x)D_h/\mu_f$	(-)
x	mass flow quality, coordinate	(-)
X	Lockhart-Martinelli parameter	(-)

Greek symbols

Δ	Difference	(-)
α	void fraction, corner half-angle	(-, °)
β	channel aspect ratio $(\beta < 1)$	(-)
ε	percentage of data points predicted within $\pm 50\%$	(%)
θ	percentage of data points predicted within $\pm 30\%$	(%)
θ_s	static contact angle	(°)
λ	mean absolute percentage error	(%)
μ	dynamic viscosity	(Ns/m^2)
ρ	density	(kg/m^3)
σ	surface tension	(N/m^2)
ϕ	two-phase flow frictional multiplier	(-)
	channel inclination angle	(°)
ω	percentage of data points predicted within $\pm 10\%$	(%)

Subscript

A	acceleration
F	frictional
G	gravitational
TP	two-phase
f	saturated liquid
g	saturated vapor
z	stream wise coordinate
fg	difference between saturated vapor and saturated liquid
fo	liquid only
go	vapor only
tt	turbulent liquid-turbulent vapor
tv	turbulent liquid-laminar vapor
vt	laminar liquid-turbulent vapor
vv	laminar liquid-laminar vapor

REFERENCES

[1] Mehdi Mortazavi and Kazuya Tajiri. Liquid water breakthrough pressure through gas diffusion layer of proton exchange membrane fuel cell. *international journal of hydrogen energy*, 39(17):9409–9419, 2014.

[2] Mehdi Mortazavi and Kazuya Tajiri. In-plane microstructure of gas diffusion layers with different properties for pefc. *Journal of Fuel Cell Science and Technology*, 11(2):021002, 2014.

[3] Anthony D Santamaria, Prodip K Das, James C MacDonald, and Adam Z Weber. Liquid-water interactions with gas-diffusion-layer surfaces. *Journal of The Electrochemical Society*, 161(12):F1184–F1193, 2014.

[4] Mehdi Mortazavi and Kazuya Tajiri. Impact of gas diffusion layer properties on liquid water breakthrough pressure in polymer electrolyte fuel cell. In *ASME 2013 11th International Conference on Fuel Cell Science, Engineering and Technology collocated with the ASME 2013 Heat Transfer Summer Conference and the ASME 2013 7th International Conference on Energy Sustainability*, pages V001T01A016–V001T01A016. American Society of Mechanical Engineers, 2013.

[5] FY Zhang, XG Yang, and CY Wang. Liquid water removal from a polymer electrolyte fuel cell. *Journal of the Electrochemical Society*, 153:A225, 2006.

[6] X. Liu, H. Guo, and C. Ma. Water flooding and two-phase flow in cathode channels of proton exchange membrane fuel cells. *Journal of power sources*, 156(2):267–280, 2006.

[7] H. Li, Y. Tang, Z. Wang, Z. Shi, S. Wu, D. Song, J. Zhang, K. Fatih, J. Zhang, H. Wang, et al. A review of water flooding issues in the proton exchange membrane fuel cell. *Journal of Power Sources*, 178(1):103–117, 2008.

[8] I.S. Hussaini and C.Y. Wang. Visualization and quantification of cathode channel flooding in pem fuel cells. *Journal of Power Sources*, 187(2):444–451, 2009.

[9] M. Mortazavi and K. Tajiri. Effect of the ptfe content in the gas diffusion layer on water transport in polymer electrolyte fuel cells (pefcs). *Journal of Power Sources*, 245:236–244, 2014.

[10] Christopher Hebling Klaus Tuber, David Pocza. Visualization of water buildup in the cathode of a transparent pem fuel cell. *J. Po*, 124:403–414, 2003.

[11] D. Spernjak, A.K. Prasad, and S.G. Advani. Experimental investigation of liquid water formation and transport in a transparent single-serpentine pem fuel cell. *Journal of Power Sources*, 170(2):334–344,

2007.

[12] EC Kumbur, KV Sharp, and MM Mench. Liquid droplet behavior and instability in a polymer electrolyte fuel cell flow channel. *Journal of Power Sources*, 161(1):333–345, 2006.

[13] XG Yang, FY Zhang, AL Lubawy, and CY Wang. Visualization of liquid water transport in a pefc. *Electrochemical and Solid-State Letters*, 7:A408, 2004.

[14] Mehdi Mortazavi and Kazuya Tajiri. Interaction between liquid droplet growth and two-phase pressure drop in pem fuel cell flow channels. In *Proceedings of the 4th International Conference of Fluid Flow, Heat and Mass Transfer*, page DOI: 0.11159/ffhmt17.133. International Academy of Science, Engineering, and Technology, 2017.

[15] JP Owejan, TA Trabold, DL Jacobson, M. Arif, and SG Kandlikar. Effects of flow field and diffusion layer properties on water accumulation in a pem fuel cell. *International Journal of Hydrogen Energy*, 32(17):4489–4502, 2007.

[16] MA Hickner, NP Siegel, KS Chen, DS Hussey, DL Jacobson, and M. Arif. In situ high-resolution neutron radiography of cross-sectional liquid water profiles in proton exchange membrane fuel cells. *Journal of the Electrochemical Society*, 155:B427, 2008.

[17] P.K. Sinha, P. Halleck, and C.Y. Wang. Quantification of liquid water saturation in a pem fuel cell diffusion medium using x-ray microtomography. *Electrochemical and Solid-State Letters*, 9(7):A344–A348, 2006.

[18] S.J. Lee, N.Y. Lim, S. Kim, G.G. Park, and C.S. Kim. X-ray imaging of water distribution in a polymer electrolyte fuel cell. *Journal of Power Sources*, 185(2):867–870, 2008.

[19] MM Mench, QL Dong, and CY Wang. In situ water distribution measurements in a polymer electrolyte fuel cell. *Journal of Power Sources*, 124(1):90–98, 2003.

[20] X.G. Yang, N. Burke, C.Y. Wang, K. Tajiri, and K. Shinohara. Simultaneous measurements of species and current distributions in a pefc under low-humidity operation. *Journal of The Electrochemical Society*, 152:A759, 2005.

[21] Mehdi Mortazavi and Kazuya Tajiri. Two-phase flow pressure drop measurement in pem fuel cell flow channels. In *ASME 2014 12th International Conference on Fuel Cell Science, Engineering and Technology collocated with the ASME 2014 8th International Conference on Energy Sustainability*, pages V001T06A011–V001T06A011. American Society of Mechanical Engineers, 2014.

[22] Hideo Ide and Hirohisa Matsumura. Frictional pressure drops of two-phase gas-liquid flow in rectangular channels. *Experimental Thermal and Fluid Science*, 3(4):362–372, 1990.

[23] Michael Grimm, Evan J See, and Satish G Kandlikar. Modeling gas flow in pemfc channels: Part i–flow pattern transitions and pressure drop in a simulated ex situ channel with uniform water injection through the gdl. *International Journal of Hydrogen Energy*, 37:12489–12503, 2012.

[24] Nathan J English and Satish G Kandlikar. An experimental investigation into the effect of surfactants on air-water two-phase flow in minichannels. *Heat transfer engineering*, 27(4):99–109, 2006.

[25] R.W. Lockhart, R.C. Martinelli. Proposed correlation of data for isothermal two-phase, two-components flow in pipes. *Chemical Eng*, 45:39–48, 1949.

[26] C. Wang, C. Chiang and D. Lu. Visual observation of two-phase flow pattern of r-22, r-134a, and r-407c in a 6.5-mm smooth tube. *Experimental Thermal and Fluid Science*, 15(4):395 – 405, 1997.

[27] D. Chisholm. A theoretical basis for the lockhart-martinelli correlation for two-phase flow. *Int. J Heat and Mass*, 10:1767–1778, 1967.

[28] K. Mishima and T. Hibiki. Some characteristics of air-water two-phase flow in small diameter vertical tubes. *International Journal of Multiphase Flow*, 22(4):703 – 712, 1996.

[29] Sira Saisorn and Somchai Wongwises. The effects of channel diameter on flow pattern, void fraction and pressure drop of two-phase airwater flow in circular micro-channels. *Experimental Thermal and Fluid Science*, 34(4):454 – 462, 2010.

[30] Mehdi Mortazavi and Kazuya Tajiri. Two-phase flow pressure drop in flow channels of proton exchange membrane fuel cells: Review of experimental approaches. *Renewable and Sustainable Energy Reviews*, 45:296–317, 2015.

[31] C.M. Hwang, M. Ishida, H. Ito, T. Maeda, A. Nakano, Y. Hasegawa, N. Yokoi, A. Kato, and T. Yoshida. Influence of properties of gas diffusion layers on the performance of polymer electrolyte-based unitized reversible fuel cells. *International Journal of Hydrogen Energy*, 36:1740, 2010.